Mon. Not. R. Astron. Soc. **276,** 1052–1066 (1995)

Studies of star formation in isolated small dark clouds – I. A catalogue of southern Bok globules: optical and *IRAS* properties

T. L. Bourke,[1]★† A. R. Hyland[1,2]†‡ and G. Robinson[1]†

[1] *Department of Physics, University College, The University of New South Wales, Australian Defence Force Academy, Canberra, ACT 2600, Australia*

[2] *Faculty of Science, The University of New South Wales, Sydney, NSW 2052, Australia*

Accepted 1995 April 12. Received 1995 April 7; in original form 1994 August 4

ABSTRACT

A comprehensive list of small southern molecular clouds (globules) has been established from the survey of southern dark clouds of Hartley et al. Only the most opaque globules, and those with diameters less than 10 arcmin, were included in the list. These are found to form an entirely complementary sample to that of Clemens & Barvainis in the northern sky.

In this and the following paper, a detailed study of the clouds is undertaken through an examination of their optical and *IRAS* properties, and radio observations of ammonia. The aim of the study is to determine their physical characteristics, their role in the formation of low-mass stars, and the physical mechanism that either triggers the star formation process or stabilizes the globules against collapse.

The globules are predominantly elliptical. There is some evidence that the apparent galactic latitude distribution of our globules (as well as that of the Clemens & Barvainis sample) is more highly concentrated towards the galactic plane than that of the large molecular cloud complexes identified through CO surveys. This suggests that there are very few high-latitude globules, or that selection effects play a major role in defining the apparent distribution.

Of the 169 globules studied, 76 are found to have *IRAS* sources lying towards them (totalling 83 sources). The *IRAS* sample is dominated by cooler sources than is the sample found to be associated with molecular cloud cores by Beichman et al., and predominantly exhibits the colours of embedded sources.

Key words: catalogues – stars: formation – stars: pre-main-sequence – ISM: clouds – infrared: stars.

1 INTRODUCTION

Bok globules (Bok & Reilly 1947) are the ideal laboratory for the study of isolated low-mass star formation. Their simple structure allows them to be modelled in detail, since the number of physical processes occurring within them is likely to be limited. As a result of their optical appearance, in particular the lack of foreground stars, the Bok globules are judged to be relatively nearby (<500 pc), and so linear scales of a few tenths of a parsec may be readily resolved with current instruments. Their isolation also means that they are relatively unaffected by the problems associated with the study of the larger, more complex molecular clouds, such as large-scale motions which may mask the smaller scale motions of direct interest, energetic H II regions, and multiple star formation within the one cloud which may destroy much of the evidence sought on the single star-forming events.

Earlier studies of Bok globules (e.g. Leung, Kutner & Mead 1982) concentrated on the larger globules (>10 arcmin), which are relatively massive and may contain multiple sites of star formation (see e.g. Beichman et al. 1984). Therefore, in order to examine single low-mass star-forming events in an isolated environment, one must turn to the smaller (<10 arcmin) isolated Bok globules. The choice

★ Present address: Harvard–Smithsonian Center for Astrophysics, 60 Garden St, MS 42, Cambridge, MA 02138, USA.
†Email: tbourke@cfa.harvard.edu (TLB); dvc@scu.edu.au (ARH); garry@phadfa.ph.adfa.oz.au (GR).
‡Present address: Office of the Vice Chancellor, Southern Cross University, Lismore, NSW 2480, Australia.

of the smallest clouds for study means that a relatively large survey may be undertaken in a reasonable number of observing sessions, using current single-dish millimetre and radio telescopes, and optical CCDs and infrared array cameras (Clemens & Barvainis 1988, hereafter CB). It also means that the largest globules in the sample (10 arcmin) will have a linear size of only 0.7 pc at a distance of 500 pc, not much larger than the typical core size found in the dark cloud complexes (~ 0.3 pc).

CB compiled a catalogue of 248 small molecular clouds located in the northern sky. In this paper we present a similar catalogue of small molecular clouds for the southern sky, with the clouds selected from the Hartley et al. (1986) catalogue. The *IRAS* Point Source Catalog (hereafter PSC) has been searched for point sources lying within the optical boundaries of the selected clouds. The optical and *IRAS* properties of the clouds are compared with those in the CB catalogue, and the *IRAS* properties of this catalogue and the CB catalogue are compared with those of the dense cores in dark cloud complexes studied by Beichman et al. (1986, hereafter Be86). Taken together, the clouds presented here and those in CB represent a unique catalogue of Bok-globule-like dark clouds.

In Paper II (Bourke et al. 1995) we describe an ammonia survey of the 169 clouds in the present catalogue, while in Paper III (Bourke et al., in preparation) we will describe the results of ammonia mapping of a number of sources and the dynamical interpretation of the ammonia observations.

2 THE SOUTHERN CATALOGUE OF SMALL ISOLATED DARK CLOUDS

The catalogue of southern dark clouds by Hartley et al. (1986) has been searched to choose a candidate set of Bok-globule-like small dark clouds for study. This catalogue, to which we shall refer as the Hartley catalogue, lists the positions of 1101 dark clouds south of $-33°$ declination. The Hartley catalogue is preferred to other southern dark cloud catalogues (e.g. Feitzinger & Stüwe 1984; Sandqvist & Lindroos 1976) as it appears to be more accurate (Hartley et al. 1986) and more comprehensive, and attempts to identify globules within complexes and not just to identify the complex. The clouds were selected on the basis of (i) opacity and (ii) size as described below. Only the most opaque (class A) clouds from Hartley were considered initially, and from this group only small clouds, or particularly opaque and obvious condensations within larger clouds, were selected, the upper limit to the cloud diameter being 10 arcmin. This upper limit also enables a complete molecular line survey of the clouds to be undertaken in a reasonable time, using beam sizes of ~ 1–2 arcmin. The search was aimed particularly at identifying *isolated* clouds satisfying the above criteria although, as indicated, for completeness the sample does include a small number of opaque clouds which appear to be connected to surrounding regions of less opaque interstellar matter, and some globular condensations within dark cloud filaments, to enable comparisons between these different types of globules. For similar reasons to those of CB, the cloud shape was not used in the selection process.

All class A clouds (432) from Hartley were inspected visually on the SERC Schmidt survey J plates for their suitability in this programme. It was found that some otherwise well-defined globules (Hyland, Bourke & Robinson 1993) had been excluded because the Hartley cloud size included low-opacity extensions to well-defined opaque clouds. All class A clouds were therefore inspected so as to avoid missing such clouds. Some clouds classified by Hartley as class B were also included in the final list after inspection of the Schmidt plates, as they satisfied our criteria for opaqueness and size. This search rendered a final survey list of 169 dark clouds satisfying the selection criteria outlined above.

Parker (1988) noted that a large number of the quoted positions of the Lynds (1962) opacity class 6 clouds are in error, or do not relate to the most opaque position within the cloud. A similar problem was found with the Hartley catalogue during this search, although to a far lesser extent. In order to check the positional accuracy of the clouds in our sample, a method similar to that employed by Parker was used. Overlays using stars from the SAO, AGK3 and Perth70 catalogues were generated for a $1\overset{\circ}{.}5 \times 1\overset{\circ}{.}5$ field about each cloud position quoted by Hartley. If the Hartley position did not correspond to either the cloud or the most opaque location within the cloud, the cloud position was remeasured with respect to the Hartley position directly from the Schmidt plate with an estimated accuracy of 30 arcsec. We were able to identify all of the class A clouds listed by Hartley, and also two clouds not previously listed. They are, using the nomenclature of Hartley, DC 322.7 + 4.0 (BHR 104; see below) and DC 322.7 + 3.9 (BHR 105). It should be noted that, unlike CB, our aim was to choose a subset of opaque clouds from the Hartley catalogue, and not to search for uncatalogued clouds. It is possible that we have not identified all clouds with sizes < 2 arcmin, which are difficult to detect at the scale of the plates (~ 1 arcmin per mm) and which make up the majority of the new clouds in the CB catalogue. On the other hand, the size distribution of the clouds in this work, when compared with that of CB (see Fig. 1 below), would suggest that not many have been missed. This may reflect a greater level of completeness to smaller sizes in the Hartley catalogue.

Table 1 lists the clouds that satisfy our selection criteria and which therefore represent our list of southern isolated small dark clouds (for convenience often referred to simply as Bok globules). Column 1 lists the cloud (BHR) number as assigned in this paper, and column 2 identifies the dark cloud (DC) name as given by Hartley. Clouds identified with an asterisk have positions that differ from those given by Hartley, the position having been remeasured. Columns 3 and 4 give the cloud's right ascension and declination in 1950.0 coordinates. Columns 5 and 6 list the major and minor axes of the clouds in arcminutes, which with few exceptions are the same as those listed by Hartley. Column 7 provides a classification of the cloud type, where I indicates that the cloud is well-isolated, and CG indicates a cometary globule, F a globule within a filament, C a globule within a less opaque complex and N a globule with an associated reflection nebula. Combinations of these types are possible, as indicated in the table. Column 8 lists other catalogued names for the clouds which we have found in the literature: CG refers to Zealey et al. (1983) and Reipurth (1983), Sa to Sandqvist & Lindroos (1976) and Sandqvist (1977), B to Barnard (1919, 1927), L to Lynds (1962) and CB to

Clemens & Barvainis (1988). Other common names and Herbig–Haro identifications are also given.

The majority of positions listed in Table 1 that are different from those of Hartley arise from the subjective determination of the cloud centre or the most opaque position within the cloud. Most of the Hartley positions for the clouds in our list do in fact lie within the cloud optical boundaries. Our remeasurements represent a personal bias in determining the optical centres of the clouds.

3 OPTICAL PROPERTIES

Our selection criteria are almost identical to those of CB, as both groups have attempted to identify the smaller (<10 arcmin) isolated Bok globules seen in the sky. In this section a comparison will be made between the optical and infrared properties of the 248 clouds included in the CB catalogue, and the 169 clouds listed in Table 1.

3.1 Cloud appearance

Of the 169 clouds in Table 1, forty are cometary-globule-like in appearance, 32 of which have been identified by Zealey et al. (1983) and Reipurth (1983) as possibly being associated with the Gum nebula.

Globules that appear as condensations within filaments account for six of the clouds, while larger clouds that appear as condensations within still larger regions of less opaque

Table 1. Catalogue of southern Bok globules, derived from the southern dark cloud catalogue of Hartley et al. (1986).

Number	DC Name	RA (1950.0) *h m s*	Dec (1950.0) ° ′ ″	*a* ′	*b* ′	Type	Other Names
1	249.7-2.1	07 56 09	−33 10 06	6	6	I	
2	251.7+0.2	08 10 29	−33 36 36	2	1	CG	CG27
3	251.8+0.0*	08 10 28	−33 46 48	1	1	CG	CG28
4	251.9+0.0	08 10 27	−33 52 00	1	1	CG	CG29
5	252.2+0.7	08 14 03	−33 41 30	2	1	CG	CG26
6	252.3+0.5*	08 13 29	−33 55 30	0.8	0.6	CG	CG33
7	252.5+0.1*	08 12 23	−34 21 08	3	1.5	CG	CG32
8	253.1-1.7A	08 07 10	−35 52 24	4	2	CG	CG31A
9	253.1-1.7B	08 06 55	−35 54 14	2	2	CG	CG31B
10	253.1-1.7C	08 06 40	−35 50 44	3	2	CG	CG31C
11	253.1-1.7D	08 06 24	−35 52 58	1	1	CG	CG31D
12	253.3-1.6	08 07 39	−35 55 54	3	2	CG	CG30/HH120
13	253.6+2.9	08 26 48	−33 35 48	5	3	CG	CG22
14	253.8-10.9	07 27 53	−41 04 12	3	1	CG	CG34
15	255.3-14.4	07 14 28	−43 52 18	2	2	CG	CG2
16	255.4−3.9	08 03 39	−39 00 18	6	2	I	
17	256.2-14.1*	07 17 49	−44 29 36	2	2	CG	CG1
18	256.9+2.6	08 35 23	−36 27 24	1	1	CG	CG36
19	257.2-10.3	07 39 16	−43 42 06	1	0.5	CG	CG5
20	259.0-13.2	07 29 05	−46 37 18	3	1	CG	CG6
21	259.4-12.7	07 32 41	−46 47 42	4	1	CG	CG4
22	259.5-16.4	07 12 50	−48 23 54	5	3	CG	CG13
23	259.9-0.0	08 33 43	−40 28 06	5	3	I/N	NGC2626
24	260.0−3.8	08 17 33	−42 45 18	1	1	CG	CG24
25	260.7-12.4	07 37 42	−47 46 12	3	1.5	CG	CG3
26	262.5-13.4	07 37 18	−49 43 48	3	1	CG	CG14
27	262.9-14.7	07 31 03	−50 39 06	3	1	CG	CG15
28	262.9-15.5	07 26 20	−50 58 18	2	1	CG	CG16
29	264.5+5.6	09 11 29	−40 17 06	5	1	I	
30	265.3-0.0	08 51 57	−44 36 36	4	2	I	Sa3
31	265.7-7.7	08 17 11	−49 34 24	3	3	I	
32	266.0+4.3	09 12 14	−42 17 36	2	1.5	CG	CG7
33	266.0-4.3*	08 35 24	−47 54 07	3	3	I/N	
34	267.2-7.2	08 25 06	−50 30 00	2	2	I	
35	267.4-0.9	08 55 45	−46 46 42	5	3	I	
36	267.4-7.5	08 24 17	−50 52 12	4	3	I/N	Sa111/HH46-47/ESO210-6a
37	267.5-7.4	08 25 12	−50 51 42	2	2	I/N	Sa112
38	267.6-6.0A*	08 32 38	−50 08 00	5	2	I/F	Sa113
39	267.6-6.0B*	08 32 49	−50 14 09	5	2	I/F	Sa113
40	267.6-6.4	08 30 31	−50 22 36	2	2	I	
41	267.7-7.4*	08 26 04	−50 59 42	5	4	I/N	
42	267.9-7.8	08 24 46	−51 29 24	3	1.5	I	
43	269.4+3.0	09 20 29	−45 36 00	3	3	I/C	Sa115
44	269.5+4.0	09 24 27	−44 58 00	8	4	I	Sa116
45	269.7-3.9	08 51 04	−50 28 42	0.5	0.5	CG	CG18

Table 1 – *continued*

Number	DC Name	RA (1950.0) h m s	Dec (1950.0) ° ′ ″	a ′	b ′	Type	Other Names
46	270.6-4.7	08 51 04	−51 40 30	1	1	CG	CG17
47	272.5+2.0	09 29 15	−48 25 06	4	2	I	
48	273.2+2.4	09 34 15	−48 40 06	6	4	I	
49	273.3+2.5	09 34 55	−48 38 24	4	3	I	
50	273.8+3.2	09 39 50	−48 27 00	7	1	I	
51	274.1+3.9	09 44 00	−48 04 18	1.5	1	CG	
52	274.1+2.7	09 39 22	−48 59 12	8	3	I	
53	274.2-0.4	09 27 05	−51 23 30	5	3	I	Sa120
54	274.3+3.4	09 43 10	−48 37 30	4	2	I	
55	275.9+1.9*	09 45 03	−50 52 29	4	3	I/C	Sa121
56	276.2-10.6	08 43 07	−59 43 06	4	3	I/N	
57	285.3-1.6	10 23 39	−59 09 54	3	2	I	
58	289.3-2.8	10 47 05	−62 07 12	3	3	I	
59	291.1-1.7	11 05 03	−61 49 36	6	3	I	Sa125
60	291.4-0.2	11 12 19	−60 36 42	4	2	I	Sa127
61	293.1+0.6	11 27 16	−60 25 54	1.5	1.5	I	
62	293.2+0.4	11 27 39	−60 41 42	3	1	I	
63	293.3+0.1	11 27 53	−60 56 48	2	1	I	
64	293.3-0.9	11 25 36	−61 53 24	3	2.5	C	Sa129
65	294.3+2.7	11 41 06	−58 45 54	3	2	I	
66	294.3-0.1	11 35 12	−61 28 00	2	1	I	
67	294.9+0.1	11 40 27	−61 27 42	2	1	I	
68	295.0+3.4	11 47 31	−58 16 24	6	4	I	Sa1
69	295.4+0.5	11 45 34	−61 09 24	3	2	I	
70	295.5+0.4	11 45 43	−61 13 54	2	2	I	
71	297.7-2.8*	11 59 03	−64 52 11	8	3	I	Sa136
72	298.3-2.8	12 04 31	−65 02 00	4	1.5	I	
73	299.6+5.6	12 23 54	−56 49 12	6	3	I	
74	300.0-3.7	12 19 21	−66 10 30	3	2	I	
75	300.2-3.5	12 21 24	−65 54 06	8	4	I	Sa139
76	300.6-3.1	12 25 27	−65 37 24	9	4	I	Sa140
77	300.7-1.0*	12 28 38	−63 28 15	6	6	C	Tapia 2
78	301.2-0.4	12 33 25	−62 56 06	5	2	I/C	Sa144
79	301.7-6.7	12 33 55	−69 14 12	7	6	I/N	Sa147
80	301.7-7.2	12 34 07	−69 43 24	7	2	CG	CG21/Sa149
81	301.7-2.6	12 36 42	−65 10 00	5	2	I/C	Sa148
82	302.0-7.0*	12 37 57	−69 35 14	4	1.5	CG	CG20/Sa151
83	302.1+7.4	12 42 48	−55 09 00	2	1	CG	CG19
84	302.6-15.9	12 40 59	−78 31 48	6	3	I/N	TPN
85	303.3+1.3	12 51 19	−61 16 48	9	4	I	Sa155
86	303.8-14.2*	13 03 41	−76 44 03	10	6	I/N	Sa160
87	307.3+2.9	13 22 34	−59 27 18	3	3	I/N	
88	314.8-5.1*	14 44 30	−65 03 24	9	5	I/N	Sa165
89	315.8-27.5A	19 02 16	−78 40 48	2	2	I/N	
90	315.8-27.5B	19 03 05	−78 40 54	3	1	I/N	
91	316.3+4.9	14 23 27	−55 14 06	4	3	I	
92	316.5+21.2*	13 54 34	−39 40 49	4	3	CG/N	CG12/NGC5367
93	316.5-4.0	14 54 09	−63 15 42	8	3	I/F	
94	316.9-4.9	15 01 00	−63 56 18	4	2	I	
95	316.9-2.1	14 49 24	−61 23 48	5	1.5	I	
96	317.0-4.6	15 00 30	−63 36 24	6	3	I	
97	319.9-4.8	15 22 59	−62 12 48	3	2	I	
98	320.1-4.3	15 22 16	−61 45 30	3	1	I	
99	320.5-3.5	15 20 56	−60 51 06	2	1	I	
100	320.5-3.6	15 21 38	−60 56 36	3	2	I	
101	320.7-1.7	15 14 51	−59 10 48	5	3	I/C	
102	320.7-2.0	15 16 16	−59 27 12	6	4	I/C	
103	320.9-2.1	15 17 35	−59 25 06	3	1	I	
104	322.7+4.0*	15 06 04	−53 19 26	1	1	I	
105	322.7+3.9*	15 06 19	−53 21 41	2	1	I	
106	323.0+4.0	15 07 34	−53 07 06	3	2	I	
107	325.2+5.8	15 13 38	−50 25 42	3	3	I	
108	325.9+5.9	15 17 27	−50 01 30	3	2	I	
109	326.8+5.6	15 22 42	−49 49 00	3	2	I	
110	326.9+5.5	15 23 27	−49 50 12	3	2	I	

Table 1 – *continued*

Number	DC Name	RA (1950.0) h m s	Dec (1950.0) ° ′ ″	a ′	b ′	Type	Other Names
111	327.2+1.8*	15 38 34	−52 38 21	10	4	I	
112	330.7-1.3*	16 09 58	−52 45 52	7	7	I	Sa178
113	331.0-0.7	16 09 00	−52 09 01	7	1	I	
114	331.1-2.3	16 16 10	−53 11 12	3	2	I	
115	332.7+6.8*	15 46 49	−45 21 24	6	2	I	
116	334.2+0.0	16 19 53	−49 26 00	3	1	I	Sa179
117	334.6+4.6	16 02 44	−45 47 12	8	5	I	
118	334.6-1.4*	16 28 10	−50 01 38	8	7	C	
119	335.9+7.0*	15 59 38	−43 09 30	7	3	I	Sa181
120	336.7+7.8	15 59 49	−41 58 12	4	3	I	
121	337.1-4.9	16 54 50	−50 31 12	8	2	I	Sa185
122	337.7-4.0	16 52 49	−49 30 54	4	4	I	Sa186
123	337.8-1.6	16 42 09	−47 54 06	6	4	I/C	
124	337.9-1.4*	16 41 13	−47 39 42	1.5	1	F	
125	338.2+0.8	16 33 02	−45 55 12	2	2	I	
126	338.6+9.5	16 01 07	−39 29 36	5	3	I	
127	338.6+11.9*	15 53 50	−37 38 30	9	5	F	Sa11/Lupus2
128	339.1+11.7A*	15 55 22	−37 31 12	4	3	F	Lupus2
129	339.1+11.7B*	15 55 47	−37 27 51	5	4	F	Lupus2
130	339.1-0.8	16 43 05	−46 22 00	2	2	I	Sa190
131	339.3-0.3	16 42 22	−45 53 24	7	5	F	Sa191
132	340.4+5.5	16 22 38	−41 08 36	3	2	I	
133	340.5+0.5	16 43 09	−44 25 24	7	2	I	Sa15
134	340.9+9.2	16 10 36	−38 09 06	7	5	I	
135	343.4+3.5	16 41 23	−40 17 36	7	2	I	Sa18
136	344.5+2.0	16 51 04	−40 26 03	1	1	CG	
137	344.6-4.3	17 18 10	−44 05 54	5	3	I/N	
138	345.0-3.5	17 16 00	−43 24 00	2	2	I	
139	345.2-3.6*	17 17 15	−43 17 30	6	5	I	
140	345.4-4.0*	17 19 18	−43 19 24	10	6	I	
141	345.8+7.6	16 33 33	−35 50 30	3	2	I	
142	346.2-11.7	17 59 18	−46 39 54	3	1.5	I	Sa193
143	346.4-5.0	17 27 02	−43 06 12	2	2	I	
144	346.4+7.9	16 34 10	−35 07 54	4	2	I	
145	347.5-8.0	17 44 23	−43 42 12	6	3	I	Sa195
146	347.9-4.4	17 28 50	−41 32 18	7	5	I	
147	348.0+3.7	16 55 04	−36 37 42	4	3	I	
148	349.0+3.0	17 01 05	−36 14 42	2.5	2.5	I	
149	349.2+3.1A	17 01 06	−36 04 18	3	1	I	
150	349.2+3.1B	17 01 25	−36 06 12	1	1	I	
151	349.3+3.1	17 01 28	−35 59 05	2	1	I	
152	351.0+3.9	17 03 22	−34 09 54	4	3	I	
153	351.2+5.1	16 59 28	−33 12 12	7	4	I	B49/Sa31/CB69
154	351.2+5.2	16 59 04	−33 12 18	2	2	I	CB69
155	351.7+0.5*	17 18 44	−35 32 29	9	5	I	Sa33
156	351.8+2.8	17 10 11	−34 11 54	2	1	I	
157	352.9+4.8	17 05 31	−32 03 00	6	3	I	B56/L1685/CB73
158	352.9+5.0	17 04 48	−31 59 00	2.5	2	I	
159	353.1+2.3	17 15 56	−33 23 48	4	2	I	
160	353.3+2.4	17 15 39	−33 12 54	2.5	2.5	I/N	
161	353.5+3.5	17 12 15	−32 21 36	3	1.5	F	
162	354.1+2.9A*	17 15 57	−32 12 48	1.5	1.5	CG	
163	354.1+2.9B*	17 15 44	−32 15 36	3	1	CG	
164	354.1+2.9C*	17 15 44	−32 12 48	3	1.5	CG	
165	354.1+2.9D*	17 16 26	−32 11 41	3	3	CG	
166	354.1+2.9E*	17 15 52	−32 08 20	4	2	CG	
167	354.2+3.2	17 15 13	−32 01 30	6	4	I/C	
168	356.5-4.5*	17 51 50	−34 13 31	4	1	I	
169	4.9-24.6	19 37 23	−34 54 36	2.5	1.5	CG	CG11

Notes.
DC Name: * indicates that the position has been remeasured.
Cloud Type: I, isolated; CG, cometary globule; N, nebula associated; F, filamentary; C, complex.
Other Names: B, Barnard (1919, 1927); CB, Clemens & Barvainis (1988); CG, Zealey et al. (1983), Reipurth (1983); L, Lynds (1962); Sa, Sandqvist & Lindroos (1976), Sandqvist (1977); Tapia 2, Tapia Coalsack globule 2 (Tapia 1973); TPN, Thumbprint nebula (FitzGerald et al. 1976).

obscuration account for only three of the clouds. The most well-known example of this type of globule is Tapia's globule 2 in the Coalsack (Tapia 1973; Jones et al. 1980; Jones, Hyland & Bailey 1984). The remaining 120 clouds appear well-isolated, although a few may be related to larger complexes (eight) or appear as well-formed globules with less opaque extensions, and others appear to form part of a filamentary chain (three), but the connections to other parts of the filament are not distinct. Nebulosities (not including the CGs) are associated with 15 of the isolated globules.

The majority of clouds in our list thus satisfy our requirement to be small *isolated* globules. Only a small number of the clouds (9 of 169) appear to be doubtful inclusions, but even they are well-formed globules. For example, the Coalsack globule 2 mentioned above is a distinct globule, but cannot be classified as truly isolated. Similarly, the filamentary globules associated with the stringy Lupus dark clouds cannot be said to be truly isolated.

3.2 Cloud sizes and shapes

Fig. 1 shows a histogram of the apparent mean optical sizes of the clouds in the two samples. The mean optical size is defined to be $\sqrt{ab}$, where a and b represent the cloud major and minor axes respectively, as listed in Table 1. The two samples have a similar distribution in cloud size. The CB sample has a peak between 2 and 4 arcmin, whilst our sample has a somewhat narrower peak between 2 and 3 arcmin. This is reflected in the mean sizes of the two samples, being 4 arcmin for the CB sample and 3 arcmin for this work.

Fig. 2 shows a histogram of the ellipticities of the two samples. Again the distributions are very similar, with the CB mean ellipticity being 2.0 and the mean of this work being 1.9. Both samples have a greatest ellipticity of about 7. Approximately 14 per cent of our sample and 16 per cent of the CB sample have ellipticities greater than 3, so the difference is not significant. It is apparent that the majority (~ 70 per cent) of the globules are not spherical (ellipticity > 1.5), and so spherical cloud models may be suitable for only about one-third of globules.

Thus Figs 1 and 2 show that the optical properties of the two samples are very similar, and so they truly represent complementary catalogues of northern and southern Bok globules.

3.3 Galactic distribution

Fig. 3 shows the combined galactic distribution of the two samples. The CB sample is represented by open circles and the present work by filled circles. The majority of clouds are seen to lie within $|b| < 10°$. Also plotted is the approximate position of Gould's Belt, the plane locating the major concentration of local O and B stars, and hence regions of extensive high-mass star formation (see e.g. Clube 1967; Westin 1985; Comerón, Torra & Goméz 1992). Hartley has noted that there is no connection between the southern dark clouds and Gould's Belt. Fig. 3 certainly shows no evidence for a connection between Gould's Belt and the galactic distribution of isolated Bok globules. Therefore we conclude that the small isolated regions of predominantly low-mass star formation are spatially distinct from the regions where most of the high-mass star formation has occurred, or is occurring, in the solar neighbourhood.

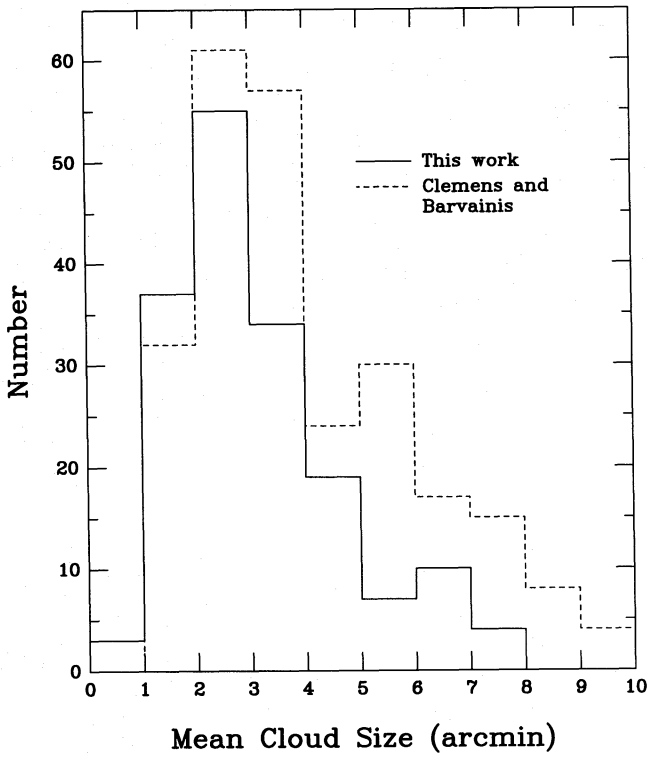

Figure 1. The distribution of the mean cloud size for the catalogued clouds. Also shown is the distribution of the CB clouds.

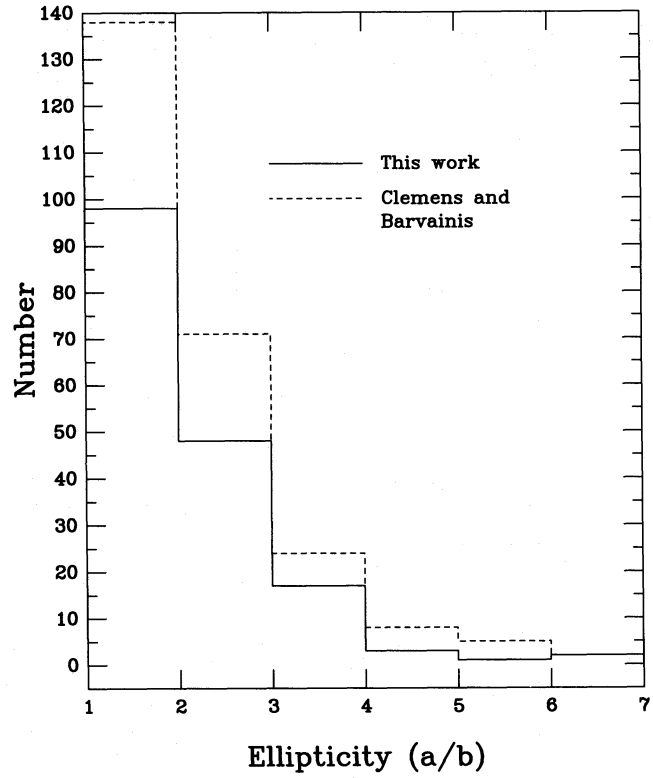

Figure 2. The distribution of the ellipticities (a/b) for the catalogued clouds and the CB sample.

The galactic distribution of the clouds in this work alone is shown in Fig. 4. Also shown are the locations of three major southern dark cloud complexes, those of Chamaeleon (I, II and III), Lupus (clouds 1–4) and the Coalsack, as well as the annulus bounding the Vela–Gum cometary globules. The two globules located in Chamaeleon are bright-rimmed globules (FitzGerald, Stephens & Witt 1976; Lehtinen et al. 1995). The dark clouds in the Lupus complex are representative of condensations within globular filaments. The Coalsack is identifiable as a large collection of globules and small clouds contained within a larger although less opaque molecular complex. The Vela cometary globule annulus, with an inner radius of ~6° and an outer radius of ~11°, centred on RA(1950) ~ 08^h18^m, Dec.(1950) ~ −44° [$(l, b) \sim (261.1, -4.5)$], is taken from Zealey et al. (1983). The vast majority of globules in Table 1 lie outside the major southern dark cloud complexes. However, globule selection was not biased against the complexes; if a dark cloud within a complex satisfied our criteria it was included.

In Fig. 5 the galactic latitude distribution of our sample is compared with that of CB. Both samples have been binned into 2° intervals, and the latitude distribution folded about

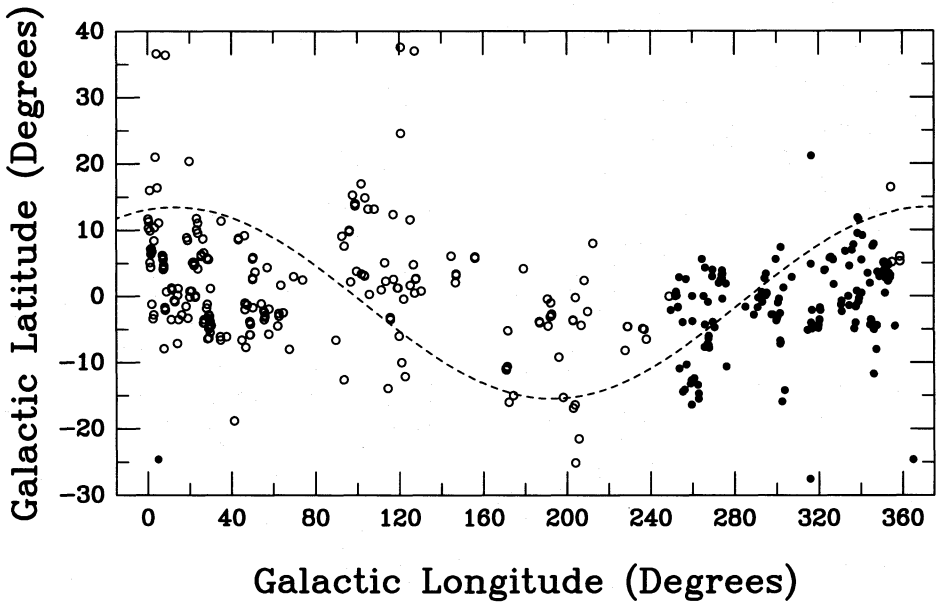

Figure 3. The galactic distribution of Bok globules from this work (filled circles) and CB (open circles). The dashed line indicates the approximate plane of Gould's Belt.

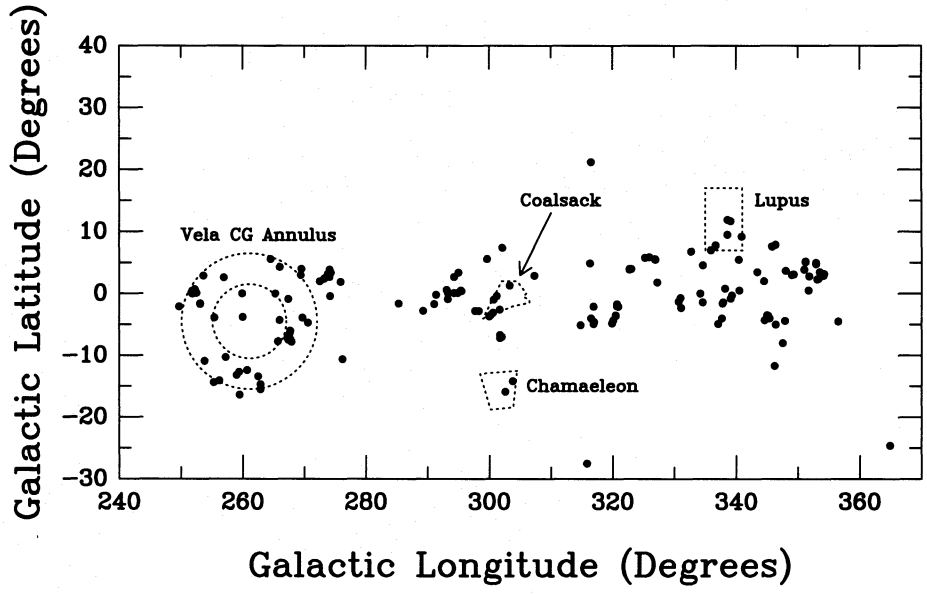

Figure 4. The galactic distribution of the clouds in this work. The three major southern dark cloud complexes of Chamaeleon, Lupus and the Coalsack are indicated, as is the annulus locating the majority of cometary globules (CGs) in the Vela–Gum complex. Note that not all the clouds in this annulus are CGs.

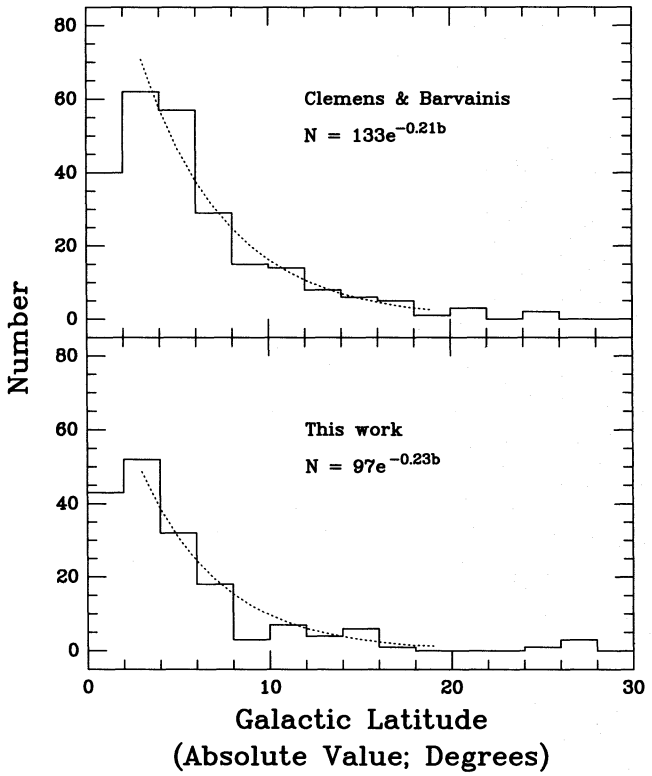

Figure 5. The galactic latitude distribution of the clouds in this work (lower panel) and CB (upper panel) binned into 2° intervals. The latitude axis has been folded about $b = 0°$. The distributions are fitted with exponential curves of the form $N = N_0 e^{-kb}$ from 2° to 20° as shown.

$b = 0°$. The distribution for the range $2° < |b| < 20°$ has been fitted with an exponential of the form $N = N_0 e^{-kb}$. The bin from 0° to 2° has been excluded, as in the CB data and also the present work there appears to be evidence for bias, resulting from the possible difficulty of identifying small globules in the galactic plane because of the increased stellar density and general interstellar extinction. We expect the majority of the sample to be nearby (< 1 kpc) because of the lack of foreground stars seen towards the clouds. It can be seen from Fig. 5 that the latitude distributions of the two samples are very similar, each having a scalewidth of ~ 4°.5. Here the scalewidth is defined as the latitude at which the number distribution falls to e^{-1} of its maximum value. We have used an exponential scalewidth in a similar fashion to the general approach taken in modelling the stellar content of the Galaxy (Bahcall & Soneira 1980). Both samples appear to be more highly concentrated towards the galactic plane than the large molecular clouds seen in CO (Clemens, Sanders & Scoville 1988). For comparison with the distribution of larger molecular clouds, we determine a FWHM scalewidth for our sample of 6°.6. CB used the assumption of similar FWHM scaleheights for the globules and the large molecular clouds to determine a mean distance to their clouds, the FWHM for the latter being 143 pc (Clemens et al. 1988). If we make the same assumption as CB of similar scaleheights for our globules and the large molecular clouds, the required mean distance of the former is ~ 1.24 kpc. This distance appears to be unrealistically large for such small optically selected dark clouds, particularly in view of the lack of foreground stars seen toward them, as has been noted above.

While the observed latitude distribution suggests that the globules are in fact more concentrated towards the galactic plane than are the large molecular clouds, it is possible that the small number of globules seen at high latitudes may be due to bias, since they are hard to identify optically in these regions because of the lack of background stars. Nevertheless, we conclude that the assumption of similar scaleheights for the large and small molecular clouds should be treated with caution when determining the globule distances. Instead, if we assume that the clouds have a similar size to the dense cores seen in CO emission of ~ 0.3 pc (Be86), and determine the mean distance required to produce the mean apparent size of ~ 3.5 arcmin for the two samples of small globules, then we find a mean distance of 300 pc for both our globule sample and that of CB. The consequence of this mean distance is that the median height above the galactic plane for the observed sample of globules is ~ 25 pc.

We have determined distances from the galactic plane for 39 sources in our sample, using globule distances derived in a variety of ways (see Paper II). These sources, which mimic the angular distribution of the complete sample, have a mean distance of 360 pc and a mean linear size (based on their individual distances and observed angular sizes) of 0.34 pc. This distance of 360 pc is remarkably similar to the result of 300 pc achieved using the assumption of a mean size of 0.3 pc for a globule sample based on the size of the CO dense cores. The median height of the 39 sources is ~ 26 pc. If this group is representative of the complete sample, which clearly needs testing, we again conclude that globules are much more concentrated towards the galactic plane than are the larger molecular clouds.

As suggested by Clemens (1994, private communication), this presents several dilemmas. He points out that a scaleheight for the globules of 25 pc would render them the most extremely concentrated of all Population I objects to the galactic plane. It is unclear how such globules could be prevented from interacting with the larger, more massive molecular cloud complexes by gravitational encounters, thereby approaching equipartition of energy with such clouds. In addition, it would be expected (unless the globules are extremely young, which does not appear to be required) that these low-mass clouds might have larger mean scaleheights than the more massive clouds. Further work clearly needs to be done to confirm or reject these findings of such a small scaleheight for the globules. One solution is to determine the distances to as many of the globules as possible on an individual basis through the tedious but preferred method of star counts (see e.g. Lynds 1968; Herbst & Sawyer 1981).

Fig. 6 shows the combined galactic longitude distribution of both samples. CB note that the strong peak at 0°–30° is most likely enhanced by the large number of background stars in this region. The peak is also seen in the 330°–360° range observed in this work for the same reason, although it is not as strong. The difference may be due to CB using both blue and red Schmidt plates to identify their clouds, since the density of background stars is likely to be greater in the red, and so identification of the smallest clouds is made easier. It

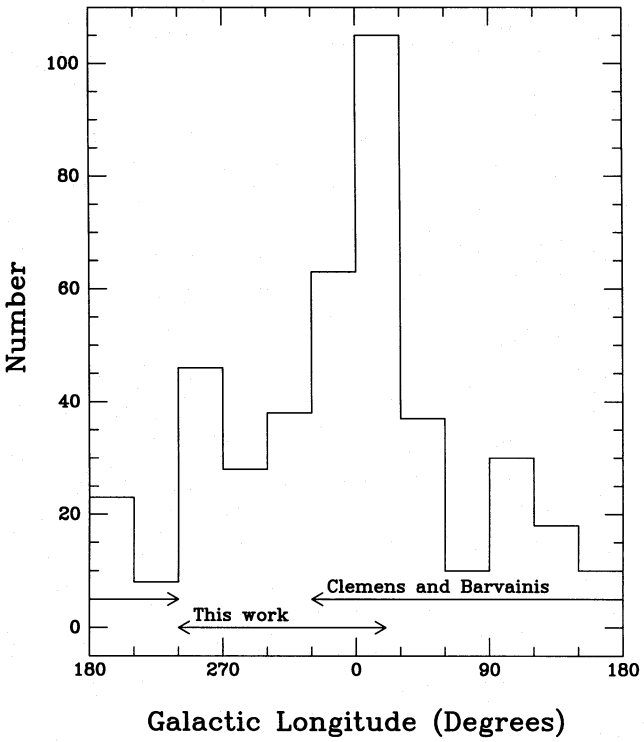

Figure 6. The combined galactic longitude distribution of the clouds in this work and CB. The regions surveyed by the two works are indicated.

may also be due to the Scorpius–Ophiuchus dark cloud lying in the 330°–360° galactic longitude range, resulting in fewer globules being distinguishable, combined with the relatively low extinction in the Scutum–Sagittarius direction enhancing the identification of globules in the 0°–30° longitude range. As a result of our latitude cutoff at −33°, however, we have not fully sampled the 330°–360° range, which will also result in an observed lack of clouds catalogued in this range.

4 *IRAS* PROPERTIES

The *IRAS* PSC was searched for sources associated with the clouds in Table 1, and comparisons made with other studies of *IRAS* point sources associated with dark clouds. For sources listed in the PSC, 'point-like' means a source with an angular size of <30 arcsec at 12 and 25 μm, <60 arcsec at 60 μm, and <120 arcsec at 100 μm (Beichman et al. 1985). The accuracy of the source positions is indicated in the PSC by a 95 per cent confidence ellipse, which for the sources in this paper is typically 30×10 arcsec^2 (semimajor × semiminor axis), but this depends on the size, brightness and spectral energy distribution of each individual source (Beichman et al. 1985).

In order to study the *IRAS* properties of their sample of dark clouds, CB defined 'core', 'envelope' and 'reference' regions for each of their clouds, where the core region was taken to be the cloud optical area, and located every *IRAS* source lying within these regions from the PSC. In this work, we have searched for *IRAS* point sources lying within the cloud's optical boundaries, and have not been concerned with envelope and reference regions. Thus we are only interested in detecting 'core' sources. The procedure used to identify the *IRAS* sources associated with the dark clouds is similar to that used by Parker (1988). For each cloud in Table 1, a search radius of 2 arcmin greater than the cloud's semimajor axis was used to locate all possible *IRAS* associations for each cloud. Such a search radius ensures that all sources lying within the optical cloud area will be detected, as well as some outside this region. No flux criteria were imposed at this stage, to enable comparison with other works which have varying criteria for the selection of *IRAS* sources (e.g. CB; Be86; Benson & Myers 1989).

The position of the *IRAS* source with respect to the cloud was then checked by generating positional overlays for each possible association, as described in Section 2, and locating the point source on the Schmidt plates. This search found 83 *IRAS* sources located within the optical boundaries of 76 clouds. Table 2 lists the *IRAS* sources found to be associated with the southern Bok globules listed in Table 1. Column 1 lists the BHR number, column 2 the dark cloud name, and column 3 the *IRAS* name, which is derived from the source's 1950.0 coordinates. Columns 4 and 5 list, respectively, the seconds of time in right ascension and seconds of arc in declination for the source. Combination of columns 3, 4 and 5 then gives the position of the *IRAS* source. Columns 6–9 give the flux in each *IRAS* waveband, with the flux detection quality in parentheses (see Section 4.1 below).

4.1 Comparison with CB associations

In this section, the properties of the *IRAS* associations are compared with those of CB, subjecting our sample to their selection criteria.

We are particularly concerned with the point-like nature of the sources (indicated by the PSC correlation flag) and the detection quality, indicated by the PSC quality flag shown in parentheses for each waveband in columns 6–9 of Table 2, where A indicates a good detection, B a moderate detection, and U an upper limit only.

4.1.1 Detection quality at 60 and 100 μm

The mean point-source correlation coefficients at 60 and 100 μm for our sources and the CB core sources are shown in Table 3. The number of sources with correlation coefficients below 95 (which indicates that the source contains some spatial structure) is also shown. From this table it is clear that the majority of sources detected at 60 and 100 μm satisfy the *IRAS* criteria of being point sources.

For similar reasons to those advanced by CB, we conclude that our clouds appear to be relatively unaffected by cirrus contamination (the two samples have identical mean values for their cirrus flags), and thus the 100-μm detections represent true globule detections.

4.1.2 Core sources

A comparison of the types of sources found in the core regions of the two samples is shown in Fig. 7. In this plot, each *IRAS* source is characterized by the band showing the *largest* detected flux. Both samples are dominated by 100-μm detections and are therefore relatively cool sources. Note,

Table 2. *IRAS* sources associated with southern Bok globules listed in Table 1.

Number	DC Name	*IRAS* Name [a]	α (sec)	δ (″)	*IRAS* flux density (Jy) [b] 12 μm	25 μm	60 μm	100 μm
22	259.5-16.4	07127-4828	46	32	0.27 (U)	0.25 (U)	0.85 (A)	5.16 (U)
22	259.5-16.4	07128-4820	51	55	0.30 (U)	0.25 (U)	0.76 (A)	6.27 (U)
15	255.3-14.4	07144-4352	28	41	0.25 (U)	0.37 (U)	0.44 (B)	8.88 (A)
17	256.2-14.1	07178-4429	54	24	6.68 (A)	7.60 (A)	13.12 (A)	33.59 (A)
27	262.9-14.7	07309-5039	58	38	0.29 (U)	0.25 (U)	0.62 (U)	6.55 (A)
26	262.5-13.4	07372-4945	13	20	0.25 (U)	0.25 (U)	0.61 (B)	8.92 (A)
25	260.7-12.4	07378-4745	50	17	0.25 (U)	0.25 (U)	1.79 (A)	13.15 (A)
19	257.2-10.3	07391-4342	06	07	0.25 (U)	0.25 (U)	0.94 (A)	4.80 (A)
12	253.3-1.6	08076-3556	40	07	0.63 (A)	3.73 (A)	18.25 (A)	47.54 (B)
3	251.8+0.0	08103-3346	22	06	0.25 (U)	0.25 (U)	0.64 (U)	5.43 (A)
2	251.7+0.2	08105-3335	32	52	0.25 (U)	0.25 (U)	0.40 (U)	4.08 (A)
7	252.5+0.1	08124-3422	29	02	0.25 (U)	0.30 (A)	11.85 (A)	40.55 (A)
5	252.2+0.7	08140-3340	04	43	0.25 (U)	0.25 (U)	0.40 (U)	3.31 (A)
31	265.7-7.7	08171-4933	11	47	0.25 (U)	0.25 (U)	0.72 (U)	13.06 (A)
36	267.4-7.5	08242-5050	16	44	0.82 (A)	6.31 (A)	26.13 (A)	58.27 (B)
34	267.2-7.2	08250-5030	03	34	0.25 (U)	0.25 (U)	1.20 (A)	17.08 (A)
41	267.7-7.4	08261-5100	11	39	0.91 (A)	2.50 (A)	4.29 (A)	10.91 (A)
13	253.6+2.9	08267-3336	44	31	0.39 (A)	1.09 (A)	3.20 (A)	14.28 (A)
23	259.9-0.0	08337-4028	42	02	0.25 (U)	39.95 (A)	347.60 (U)	1266.00 (B)
23	259.9-0.0	08337-4024	43	40	0.47 (A)	0.90 (A)	2.31 (U)	35.21 (U)
18	256.9+2.6	08354-3626	24	09	0.25 (U)	0.25 (U)	0.70 (A)	5.44 (A)
56	276.2-10.6	08433-5945	22	06	0.32 (U)	0.18 (A)	1.83 (A)	9.74 (B)
47	272.5+2.0	09293-4824	21	57	0.25 (U)	0.28 (U)	0.46 (U)	3.03 (A)
54	274.3+3.4	09430-4838	02	59	0.25 (U)	0.25 (U)	0.40 (U)	3.30 (A)
55	275.9+1.9	09449-5052	57	06	0.25 (U)	0.27 (U)	8.16 (A)	22.30 (A)
58	289.3-2.8	10471-6206	07	22	0.25 (U)	0.27 (B)	5.36 (A)	37.11 (A)
67	294.9+0.1	11403-6126	23	47	0.60 (U)	0.52 (A)	3.57 (A)	43.91 (B)
71	297.7-2.8	11590-6452	03	11	0.25 (U)	6.53 (A)	77.38 (A)	192.90 (A)
73	299.6+5.6	12239-5649	54	46	0.25 (U)	0.25 (U)	0.76 (U)	6.16 (A)
79	301.7-6.7	12345-6910	32	33	1.07 (A)	2.41 (A)	4.44 (A)	14.63 (U)
81	301.7-2.6	12369-6509	56	10	0.37 (A)	0.25 (U)	0.92 (U)	11.99 (U)
83	302.1+7.4	12427-5508	43	38	0.25 (U)	0.25 (U)	2.23 (A)	12.17 (A)
86	303.8-14.2	13036-7644	41	03	0.25 (U)	1.05 (A)	6.38 (A)	22.57 (A)
87	307.3+2.9	13224-5928	26	07	1.20 (A)	2.35 (A)	8.19 (A)	37.21 (A)
92	316.5+21.2	13546-3941	41	45	0.47 (B)	1.13 (A)	0.40 (U)	201.90 (U)
92	316.5+21.2	13547-3944	42	07	7.81 (A)	8.94 (A)	67.49 (A)	201.90 (A)
88	314.8-5.1	14437-6503	43	30	0.40 (A)	0.25 (U)	0.67 (U)	44.64 (U)
88	314.8-5.1	14451-6502	07	55	1.26 (A)	1.46 (A)	4.66 (A)	22.71 (B)
106	323.0+4.0	15075-5307	33	34	0.25 (U)	0.25 (U)	0.67 (U)	11.34 (A)
106	323.0+4.0	15075-5308	33	56	0.43 (A)	0.26 (A)	1.58 (A)	7.82 (U)
107	325.2+5.8	15133-5025	23	42	0.25 (U)	0.65 (U)	0.42 (U)	8.46 (A)
101	320.7-1.7	15148-5911	52	23	1.33 (U)	1.15 (A)	10.69 (A)	123.50 (U)
99	320.5-3.5	15210-6051	00	51	0.25 (U)	0.25 (U)	1.43 (B)	12.31 (A)
100	320.5-3.6	15215-6056	32	19	0.25 (U)	0.49 (A)	3.39 (A)	16.55 (A)
98	320.1-4.3	15223-6146	21	04	0.25 (U)	0.25 (U)	2.01 (A)	11.59 (B)
109	326.8+5.6	15227-4948	42	55	0.25 (U)	0.25 (U)	0.46 (U)	7.09 (A)
97	319.9-4.8	15230-6211	00	52	0.25 (U)	0.20 (B)	2.01 (A)	15.38 (A)
110	326.9+5.5	15233-4949	22	46	0.25 (U)	0.25 (U)	0.40 (U)	6.78 (A)
115	332.7+6.8	15468-4521	53	45	0.25 (U)	0.27 (U)	0.47 (U)	7.89 (A)
126	338.6+9.5	16009-3927	55	56	1.27 (A)	0.44 (B)	0.58 (U)	6.56 (B)
117	334.6+4.6	16029-4548	57	08	1.56 (A)	1.10 (A)	1.04 (U)	49.54 (U)
112	330.7-1.3	16097-5247	45	03	0.83 (A)	1.06 (U)	5.92 (U)	49.95 (B)
118	334.6-1.4	16277-5001	46	41	1.35 (A)	3.68 (U)	3.82 (B)	99.48 (U)
118	334.6-1.4	16282-5002	15	27	6.80 (U)	4.30 (U)	2.45 (A)	304.00 (U)
125	338.2+0.8	16328-4553	53	59	4.04 (U)	5.05 (U)	35.59 (U)	323.00 (A)
131	339.3-0.3	16415-4550	33	07	2.15 (A)	1.82 (A)	11.07 (A)	222.30 (U)
136	344.5+2.0	16510-4026	05	47	0.96 (A)	1.68 (B)	15.87 (B)	56.80 (U)
121	337.1-4.9	16549-5030	59	58	0.41 (A)	0.28 (U)	0.63 (U)	12.21 (B)
121	337.1-4.9	16554-5031	27	00	0.36 (U)	0.84 (A)	1.98 (A)	48.65 (U)
154	351.2+5.2	16590-3313	01	14	0.80 (B)	1.30 (A)	1.75 (U)	8.82 (U)
153	351.2+5.1	16594-3315	25	08	2.71 (A)	2.92 (A)	0.88 (U)	10.02 (U)
153	351.2+5.1	16595-3311	31	15	1.61 (A)	1.49 (A)	1.45 (U)	26.75 (A)

Table 2 – *continued*

Number	DC Name	*IRAS* Name [a]	α (sec)	δ (″)	*IRAS* flux density (Jy) [b] 12 μm	25 μm	60 μm	100 μm
148	349.0+3.0	17011-3613	09	59	0.37 (B)	0.54 (A)	4.50 (A)	35.59 (A)
149	349.2+3.1A	17012-3603	12	10	0.30 (U)	0.89 (A)	5.31 (A)	30.70 (A)
150	349.2+3.1B	17014-3606	30	17	0.45 (U)	0.39 (U)	5.79 (A)	25.77 (U)
151	349.3+3.1	17015-3559	35	01	3.25 (A)	1.64 (A)	3.69 (A)	23.92 (U)
158	352.9+5.0	17048-3158	49	52	0.41 (U)	0.30 (U)	2.84 (U)	17.32 (A)
157	352.9+4.8	17056-3204	39	26	0.42 (A)	0.44 (U)	2.81 (U)	16.70 (A)
156	351.8+2.8	17102-3411	12	55	1.04 (U)	1.83 (U)	2.93 (A)	42.10 (U)
161	353.5+3.5	17122-3222	17	06	1.55 (U)	0.36 (U)	3.25 (A)	22.46 (U)
167	354.2+3.2	17151-3202	08	24	1.65 (U)	1.05 (B)	10.81 (A)	43.68 (B)
160	353.3+2.4	17156-3312	36	45	1.55 (U)	1.75 (U)	15.31 (A)	71.84 (A)
164	354.1+2.9C	17157-3212	42	58	1.12 (A)	3.11 (A)	16.61 (A)	44.17 (U)
138	345.0-3.5	17159-4324	54	04	0.50 (U)	0.30 (U)	2.72 (A)	48.22 (U)
159	353.1+2.3	17159-3324	55	16	0.64 (B)	3.82 (A)	16.13 (A)	278.50 (U)
139	345.2-3.6	17169-4314	56	39	0.25 (U)	0.72 (U)	3.18 (U)	23.99 (A)
139	345.2-3.6	17172-4316	15	54	0.39 (A)	0.78 (A)	4.18 (B)	29.01 (A)
137	344.6-4.3	17181-4405	09	48	2.65 (A)	3.63 (A)	59.88 (A)	170.00 (B)
155	351.7+0.5	17187-3531	45	57	1.83 (A)	3.48 (U)	99.61 (U)	446.60 (U)
140	345.4-4.0	17193-4319	18	24	0.25 (U)	0.68 (A)	4.74 (A)	22.98 (A)
140	345.4-4.0	17195-4320	30	07	0.54 (A)	0.96 (U)	4.74 (U)	25.43 (U)
168	356.5-4.5	17518-3414	54	03	0.44 (U)	0.37 (U)	1.40 (B)	15.85 (A)
89	315.8-27.5A	19025-7840	30	39	0.25 (U)	0.25 (U)	0.40 (U)	4.36 (A)

Notes.
[a] Column 3 lists the *IRAS* name, which is derived from the source's 1950.0 coordinates specified in hours, minutes and tenths of minutes of right ascension, and degrees and minutes of declination. Columns 4 and 5 list respectively the seconds of time in right ascension and seconds of arc in declination for the source. Combination of columns 3, 4 and 5 then gives the position of the *IRAS* source.
[b] Values in parentheses indicate the quality of the detection, where A indicates a good detection, B a moderate detection, and U an upper limit.

Table 3. Detection quality of 60- and 100-μm sources in this work and CB. CORR1 refers to the *IRAS* PSC correlation flag, indicating the point-like nature of the source. Values of CORR1 below 95 indicate that some spatial structure is present. The values in parentheses indicate the sample standard deviation.

λ (μm)	Number of Sources		Mean CORR1		CORR1 < 95	
	This Work	CB	This Work	CB	This Work	CB
60	52	56	98.6 (1.6)	98.2 (2.2)	1	6
100	56	74	98.5 (1.7)	98.2 (1.7)	1	2

however, that ~28 per cent of the CB sources are characterized by such 12-μm detections, while only ~6 per cent of the current sample have such detections. Our distribution is almost totally 60- and 100-μm-dominated (~89 per cent) without correcting each band for the number of chance associations, while the corresponding number for the CB sample is ~66 per cent. If the 12-μm-dominant sources are removed from both samples (i.e. if only the 25-, 60- and 100-μm-dominant sources are considered), the percentages in the two samples become virtually identical. Reasons for excluding the 12-μm-dominant sources are given below.

Sources that have $S_{12} \geq S_{25}$ (where S_i is the flux in janskys at the wavelength i in microns) when detected in both wavebands, or that have 12-μm detections only, are most likely to be stars. This includes a few sources that have S_{60} or $S_{100} > S_{12}$. CB found that 41 of their 145 core sources have

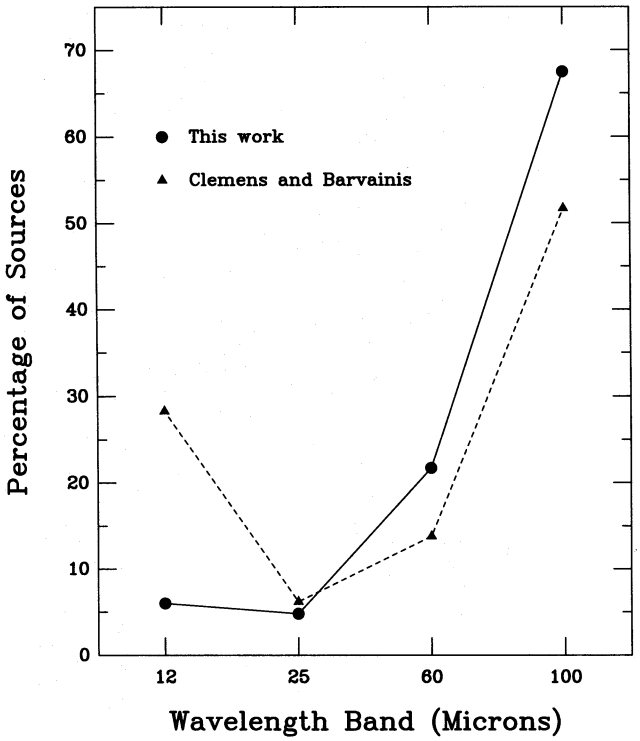

Figure 7. Normalized distribution of *IRAS* PSC detections located within the optical boundaries of the clouds of this work and CB, versus the band containing the dominant detection. Both samples are dominated by 100-μm sources.

these flux characteristics (~28 per cent), while the present work contains only 10 such sources (~12 per cent). CB conclude from the galactic distribution of these *IRAS* sources (peaked strongly between 0° and 30° in longitude; see Fig. 6) that the majority of them are obscured background giant stars in the galactic bulge. Our smaller sample is peaked between 320° and 360°, which would also indicate that these stellar-like sources are most likely background giant stars. Of the 10 sources, four have possible optical counterparts and so may be foreground stars. We have seen for the CB dark cloud sample that the galactic longitude distribution is peaked between 0° and 30°, as is the *IRAS* sample characterized by detections in the two shortest wavebands.

The large density of background stars in this longitude range, mainly as a result of the atypical low extinction in the direction of Scutum–Sagittarius, is the most likely reason for both of these peaks. As mentioned above, CB found a large number of their clouds in the range 0°–30° (104), while in the range 330°–360° we find 57 clouds. This asymmetry around the Galactic Centre may be significant, although our selection criteria mean that we have not fully sampled this longitude range. There does not appear to be any bias in the *IRAS* catalogue in longitude about the Galactic Centre. We suggest that the difference may (in addition to the sampling mentioned above) be due to the presence of the above-mentioned abnormally low extinction in the 0°–30° longitude range, enhancing the identification of small clouds in that part of the sky. While this would explain part of the increase in the number of *IRAS* identifications with globules in this region, it cannot of itself explain the greatly increased fraction of identifications compared with those in the 330°–360° region.

CB define warm *IRAS* cores to be those with $S_{25} > S_{12}$ or 25-μm detections only, of which they found eight (6 per cent), while in the present work there are four such sources (5 per cent). In neither sample is there a source that shows detected $S_{60} \gtrsim S_{100}$, although CB found 21 sources (14 per cent) with detections at 60 μm that had larger 100-μm upper limits, compared with 15 (21 per cent) for this work. In both samples the majority of sources are cool, i.e. $S_{100} \gtrsim S_{60}$ (52 per cent for CB, 65 per cent for this work).

Following CB, the globules may be divided into two categories, bright and dark where bright globules are those with bright rims (such as the cometary globules) or that contain embedded reflection nebulosity. We shall refer to the bright globules as bright-rim globules to avoid later confusion with bright *IRAS* sources [as defined by their $\log(S_{100})$ value]. For the clouds in this work, 33 *IRAS* point sources were detected toward 55 bright-rim globules (60 per cent) and 50 toward 114 dark globules (44 per cent). For CB, the corresponding figures are 22 of 31 (71 per cent) for bright-rim globules and 87 of 217 (40 per cent) for dark globules. For the bright-rim globules in our work that are not labelled 'CG' in Table 1, we find 13 point sources toward 15 clouds (87 per cent). Thus these sources with reflection nebulosities are very highly correlated with *IRAS* point sources, and would therefore appear to be excellent indicators of the sites of star formation. The cometary globules themselves, with 20 detections from 40 CGs (50 per cent), are intermediate in their detection percentages.

4.2 Comparison with Be86 associations

In this section a comparison is made between the *IRAS* sources in this work and those of CB and Be86.

Be86 searched for *IRAS* sources associated with a sample of molecular cores embedded in larger cloud complexes, where the cores are defined by their emission in CO or NH_3 as well as by their optical appearance. These cores come from the lists of Myers, Linke & Benson (1983) and Myers & Benson (1983). Be86 required that their *IRAS* associations have detections in the 25-μm band, or in both the 60- and 100-μm bands, in an attempt to exclude 12-μm-only sources (stars) and 100-μm-only sources (which may be contaminated by cirrus). In order to compare all three samples, in this section the selection criteria of Be86 have been applied to the sources in Table 2 and in CB.

Fig. 8 shows a $\log(S_{12}/S_{25})$ versus $\log(S_{25}/S_{60})$ colour–colour space plot for the *IRAS* sources from this work that have been detected at 12, 25 and 60 μm, and also those of CB and Be86. Fig. 9 shows a $\log(S_{25}/S_{60})$ versus $\log(S_{60}/S_{100})$ plot of sources detected in the 25-, 60- and 100-μm bands for the three samples. On both plots, regions defined empirically by Emerson (1987) to represent the *IRAS* colour–colour space occupied by T Tauri stars are shown. The Be86 sources on average populate a preferentially warmer region than the CB sample or the sources in this work, and contain a larger fraction of T Tauri stars. It would appear that the *IRAS* sources found in globules tend to be cooler than the sources found in the dense cores of the dark cloud complexes. This may suggest that the pre-main-sequence population in dark cloud complexes has a larger age spread than that found in globules. The bright-rim sources in the present work appear to occupy a warmer region in $\log(S_{60}/S_{100})$ space than the dark sources.

Emerson also defined an embedded sources region, based on those associations in Be86 that do not possess an optical

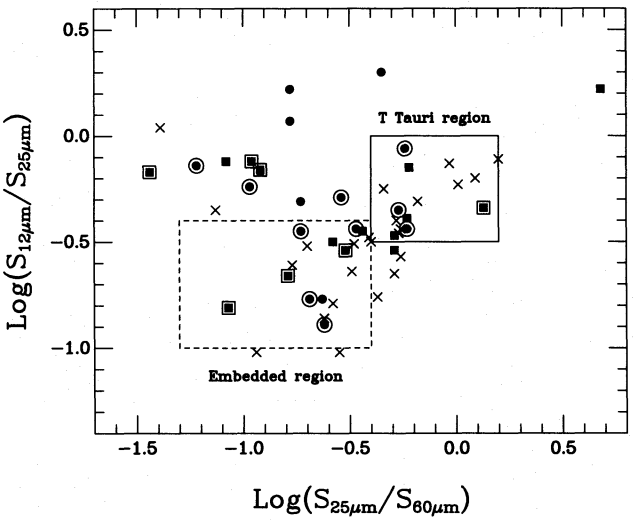

Figure 8. The distribution in 12–25–60 μm colour–colour space for the sources in this work (circles), CB (squares) and Be86 (crosses). Also indicated in the plot are the regions occupied by known T Tauri stars and embedded sources. The sources in this work and CB that are associated with nebulosity are indicated by the points with haloes.

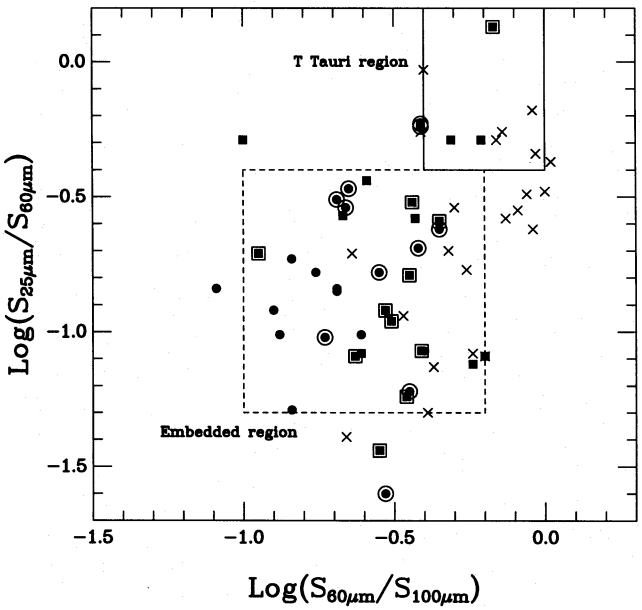

Figure 9. As for Fig. 8, but showing the 25–60–100 μm colour–colour space distribution.

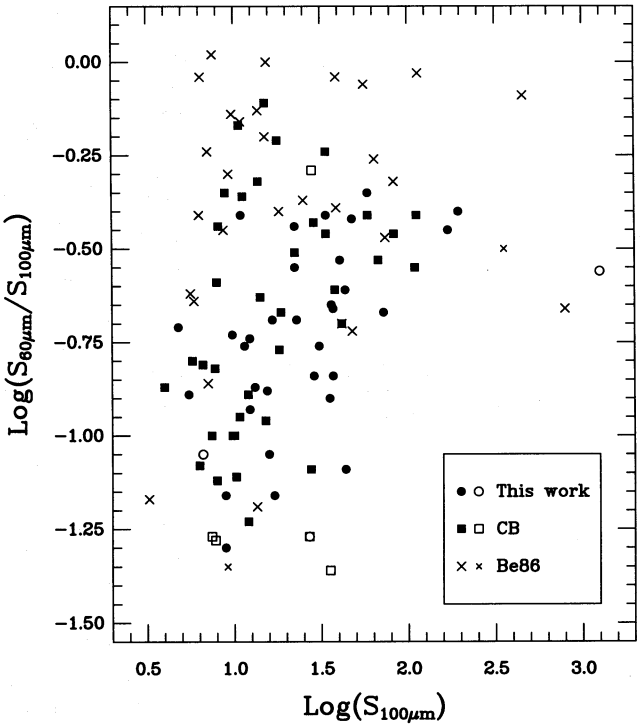

Figure 10. The 60–100 μm colour–magnitude distribution for sources in this work, CB and Be86. This plot indicates that the brighter sources are warmer, and that the Be86 sources are warmer than the CB sources or the sources in this work. The open symbols (this work and CB) and the two small crosses (Be86) represent sources with upper limits only at 60 μm.

counterpart. As has been seen, the $\log(S_{60}/S_{100})$ colours of the Be86 sample indicate that their sources are warmer than the CB sample and the associations in the present work. It would seem that the Be86 sample does not probe the coldest *IRAS* sources associated with dark clouds, and so the embedded sources region in colour–colour space defined by the Be86 associations does not reflect the true distribution of known embedded sources in all dark clouds. The Be86 embedded sources lie in the range $-0.7 \lesssim \log(S_{60}/S_{100}) \lesssim 0.0$, while Fig. 9 shows that the majority of globules of CB and the present work occupy a region bounded by $-1.0 \lesssim \log(S_{60}/S_{100}) \lesssim -0.2$. As a result, the empirically defined region for the known embedded sources in globules is taken to be

$$-1.0 \lesssim \log(S_{12}/S_{25}) \lesssim -0.4,$$

$$-1.3 \lesssim \log(S_{25}/S_{60}) \lesssim -0.4,$$

$$-1.0 \lesssim \log(S_{60}/S_{100}) \lesssim -0.2.$$

The embedded regions are shown in Figs 8 and 9. Note that in both plots very few of our sources fall into the T Tauri region. It is thought that those sources occupying the Be86 embedded region are the best 'protostellar' candidates to be found in the PSC (Be86; Myers et al. 1987; Parker 1991). This is probably also true for our somewhat more extended embedded region.

Fig. 10 shows the $\log(S_{60}/S_{100})$ versus $\log(S_{100})$ plot for the three samples. The distribution of CB sources in this plot is similar to the present work. All three samples indicate that the brighter sources [as defined by their $\log(S_{100})$ values] are warmer [as defined by their $\log(S_{60}/S_{100})$ ratios]. It is interesting to note that there are no bright sources [$\log(S_{100}) > 2.0$] with $\log(S_{60}/S_{100}) < -0.75$, while there are many fainter sources with 'warm' 60–100 μm colours. Note that one of our sources is very bright at 100 μm, with a value of $\log(S_{100}) > 3$.

The temperature of the emitting dust has been estimated by fitting a greybody modified by a power emissivity law of the form $\lambda^{-\beta}$ to the 60- and 100-μm fluxes. The dust temperatures derived in this manner for the three samples are shown in Table 4, assuming various values of β. The value of $\beta = 0$ corresponds to the dust grains acting purely as a greybody, while $\beta = 2$ corresponds to crystalline grains. Table 4 again shows that the Be86 sample is warmer and that the dust temperatures of the CB sample and this work are almost identical.

A comparison of the mean 100-μm fluxes of the three samples shows that the Be86 sample is brighter in the far-infrared. The mean 100-μm flux of the Be86 sample is 80 ± 30 Jy, that of the CB sample 25 ± 5 Jy and that of this work is 34 ± 7 Jy (excluding the source with $S_{100} > 1000$ Jy). As yet we have not been able to arrive at a completely satisfactory thesis as to why the Be86 sources are warmer *and* yet brighter at 100 μm. If the distance estimates are reasonable then the Be86 sources are, on the average, closer than the two samples of globules, and this may explain their larger apparent brightness at 100 μm. The fact that they are warmer in $\log(S_{60}/S_{100})$ may be due to them being older, more massive or less embedded, or perhaps they possess more circumstellar material.

Finally, Fig. 11 plots the distribution of 100-μm fluxes for the sources detected at this wavelength by CB (upper panel) and our sample (lower panel). In the upper plot the dashed line represents the best fit to the upper four flux bins, while in the lower plot the fit is to the upper six flux bins. The PSC is

Table 4. Mean dust temperatures of *IRAS* sources based on *IRAS* 60–100 μm colours, where the emissivity is assumed to follow a power law of the form $\lambda^{-\beta}$. The range of temperature for each sample is indicated in square brackets.

β	T_d (60–100) (K)		
	Be86	CB	This work
0	42 [22–69]	32 [22–56]	32 [21–42]
1	34 [20–49]	27 [20–42]	27 [19–34]
2	29 [18–39]	24 [18–34]	24 [17–29]

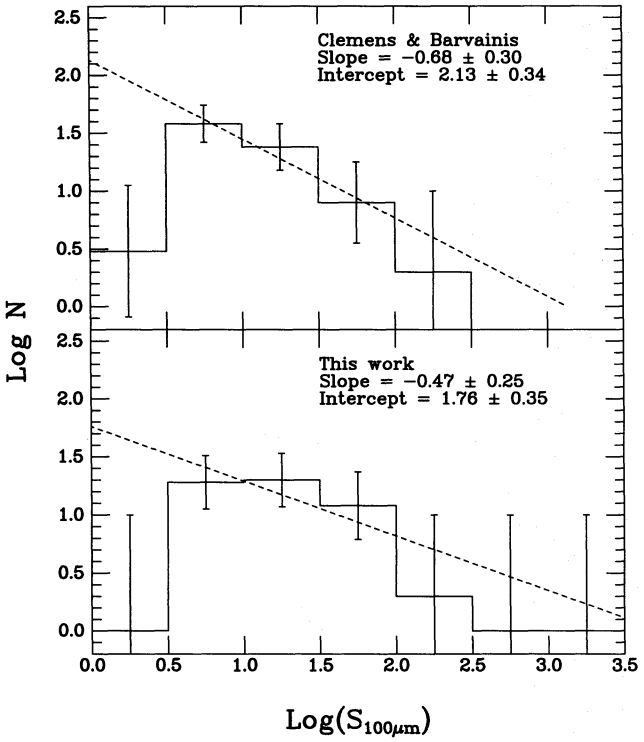

Figure 11. The *IRAS* 100-μm detected flux distribution for CB (upper panel) and this work (lower panel). In the upper panel the dashed line represents the best fit to the upper four flux bins [i.e. $\log(S_{100})=0.5$–2.5], while in the lower plot the fit is to the upper six flux bins [i.e. $\log(S_{100})=0.5$–3.5].

incomplete below 3 Jy [$\log(S_{100})=0.5$], which is reflected in the size of the first flux bin, i.e. only one source was detected below this value in the present work, and three by CB. If the PSC were complete down to 1 Jy [$\log(S_{100})=0$] and the same fits were to apply, then the total number of clouds detected at 100 μm in the CB sample would be ~66 per cent, while for the clouds in this work it would be ~57 per cent. A comparison of the two plots in Fig. 11 indicates that bin 2 [$\log(S_{100})=0.5$–1.0] for our sample may also be incomplete. If bin 2 for our sample were incomplete and the same fit were to apply, then 63 per cent of our clouds would have been detected. Clemens, Yun & Heyer (1991) have shown with the use of co-added *IRAS* survey data that the cloud detection rate is almost 100 per cent down to the 1-Jy level for the CB clouds. As noted by CB, the clouds with detections below 3 Jy may represent the most quiescent clouds in the sample, i.e. those that are not forming stars. The identification and study of these clouds is important in the overall investigation of the star formation process in Bok globules.

5 SUMMARY AND CONCLUSIONS

As the initial phase of our studies of star formation in isolated small dark clouds, the catalogue of southern dark clouds by Hartley et al. (1986) has been searched for a candidate set of Bok globules satisfying the criteria that they be small (<10 arcmin), optically dense and generally isolated from bright nebulosities and other dark clouds. This has resulted in a final list of 169 small dark clouds, the majority of which have not previously been studied in any form.

The major results of this investigation are as follows.

(i) The positions quoted by Hartley were found to be very reliable in locating the densest positions within the clouds, with minor revisions necessary in only a small number of cases. This can be compared with the Lynds catalogue of northern dark clouds (Lynds 1962), where numerous discrepancies have been found for the quoted positions of the smallest clouds in the list (see e.g. Parker 1988).

(ii) The optical properties of the Bok globules in this work are very similar to those of the globules catalogued by Clemens & Barvainis (1988). The two samples have very similar mean sizes (3 arcmin compared with 4 arcmin) and ellipticities (1.9 compared with 2.0, with a greatest ellipticity of 7 in both samples). Both samples include globules of a wide range of shape which may indicate differences in the rotational and magnetic properties of the clouds.

(iii) The major dark cloud complexes in the southern sky, those of Chamaeleon, Lupus and the Coalsack, are represented in the catalogue, although the vast majority of the sample are well-isolated from these complexes. By combining the two catalogues (CB and this work) it has been shown that there is no correlation between the Bok globules (sites of predominantly low-mass star formation) and Gould's Belt (which contains many of the regions responsible for the majority of high-mass star formation in the solar neighbourhood). This lack of correlation supports the view that these two manifestations of star formation are to a large extent spatially distinct.

(iv) The galactic distribution reveals some interesting features about the globules which are yet to be fully understood. The latitude distribution has an exponential scale-width of only 4°.5, which suggests that, at the mean distance we have derived on the basis of an assumed mean cloud size of 0.3 pc, the median height above the plane is only ~25 pc. A remarkably similar value is obtained by the detailed analysis of 39 sources, for which the distances are reasonably well-established. A scaleheight of only 25 pc may be compared with the scaleheight of 143 pc for the large molecular clouds seen in CO, and raises several unresolved difficulties.

The longitude distribution shows an interesting asymmetry with respect to the Galactic Centre. While part of this may be attributed to factors such as the Ophiuchus dark cloud complex diminishing the numbers of isolated globules identified in the 330°–360° region, and part to the atypical low extinction in the direction of Scutum–Sagittarius

enhancing the number of isolated globules in the 0°–30° region, the magnitude of the effect remains to be understood.

(v) The list includes ~40 cometary globules, the majority of which are associated with the Vela–Gum complex. These may represent an early stage in the formation of isolated Bok globules (Reipurth 1983; Leung 1985).

(vi) A total of 83 *IRAS* associations have been found toward 76 of the clouds (~45 per cent). A comparison with the *IRAS* sources associated with the CB catalogue shows that the properties of the two samples are very similar. Both samples are dominated by sources with 60- and 100-μm detections and therefore consist primarily of cool sources.

(vii) A comparison of these two samples with the work of Be86 shows that the isolated Bok globules are cooler and not as bright in the far-infrared as the dense cores located within larger cloud complexes. The majority of *IRAS* associations in this work detected at 60 and 100 μm are located in the embedded region of 25–60–100 μm colour–colour space. This group of associations represent a candidate set of 'protostellar' objects and thus deserve closer study.

(viii) The PSC is incomplete below 3 Jy at 100 μm. If this detection limit could be lowered to 1 Jy then a large percentage of Bok globules in this work and CB would have been detected by *IRAS* in its longest waveband. Clemens et al. (1991) have shown with the use of co-added *IRAS* data that the detection rate is almost 100 per cent for the CB sample. The globules with detections below 3 Jy represent a quiescent class of globules which are not likely to be forming stars at the present time (CB) and therefore deserve closer attention.

The catalogue presented here represents the ideal starting point for a study of low-mass star formation within small southern molecular clouds. In the following paper, we present the results of an ammonia survey of the molecular clouds in this catalogue.

ACKNOWLEDGMENTS

We thank Steve James for computing assistance associated with the use of the machine-readable version of the *IRAS* PSC, and Mt Stromlo and Siding Spring Observatories for access to their Schmidt plates and computing facilities. We acknowledge the many suggestions of the referee, Dr D. P. Clemens, particularly those related to the derived scaleheight of the globules and the nature of the Be86 sources, which we believe have led to a significant improvement in this paper. This project has been supported in part by a grant from the Australian Research Council. One of us (TLB) thanks the Department of Physics, ADFA, for financial assistance during part of this study.

REFERENCES

Bahcall J. N., Soneira R. M., 1980, ApJS, 44, 73
Barnard E. E., 1919, ApJ, 49, 1
Barnard E. E., 1927, Frost E. B., Calvert M. R., eds, A Photographic Atlas of Selected Regions of the Milky Way, Carnegie Inst., Washington, DC
Beichman C. A. et al., 1984, ApJ, 278, L45
Beichman C. A., Neugebauer G., Habing H. J., Clegg P. E., Chester T. J., eds, 1985, *IRAS* Catalogs and Atlases, Vol. 1, Explanatory Supplement. US Government Printing Office, Washington, DC
Beichman C. A., Myers P. C., Emerson J. P., Harris S., Mathieu R., Benson P. J., Jennings R. E., 1986, ApJ, 307, 337 (Be86)
Benson P. J., Myers P. C., 1989, ApJS, 71, 89
Bok B. J., Reilly E. F., 1947, ApJ, 105, 255
Bourke T. L., Hyland A. R., Robinson G., James S. D., Wright C. M., 1995, MNRAS, 276, 1067 (Paper II, this issue)
Clemens D. P., Barvainis R., 1988, ApJS, 68, 257 (CB)
Clemens D. P., Sanders D. B., Scoville N. Z., 1988, ApJ, 327, 139
Clemens D. P., Yun J. L., Heyer M. H., 1991, ApJS, 75, 877
Clube S. V. M., 1967, MNRAS, 137, 189
Comerón F., Torra J., Goméz A. E., 1992, Ap&SS, 187, 187
Emerson J. P., 1987, in Peimbert M., Jugaku J., eds, Proc. IAU Symp. 115, Star Forming Regions. Reidel, Dordrecht, p. 19
Feitzinger J. V., Stüwe J. A., 1984, A&AS, 58, 365
FitzGerald M. P., Stephens T. C., Witt A. N., 1976, ApJ, 208, 709
Hartley M., Manchester R. N., Smith R. M., Tritton S. B., Goss W. M., 1986, A&AS, 63, 27
Herbst W., Sawyer D. L., 1981, ApJ, 243, 935
Hyland A. R., Bourke T. L., Robinson G., 1993, in Soifer B. T., ed., ASP Conf. Ser. Vol. 43, Sky Surveys: Protostars to Protogalaxies. Astron. Soc. Pac., San Francisco, p. 49
Jones T. J., Hyland A. R., Robinson G., Smith R. G., Thomas J., 1980, ApJ, 242, 132
Jones T. J., Hyland A. R., Bailey J., 1984, ApJ, 282, 675
Lehtinen K., Mattila K., Schnur G. F. O., Prusti T., 1995, A&A, 295, 487
Leung C. M., 1985, in Black D. C., Matthews M. S., eds, Protostars and Planets II. Univ. Arizona Press, Tucson, p. 104
Leung C. M., Kutner M. L., Mead K. N., 1982, ApJ, 262, 583
Lynds B. T., 1962, ApJS, 7, 1
Lynds B. T., 1968, in Middlehurst B. M., Aller L. H., eds, Nebulae and Interstellar Matter. Univ. Chicago Press, Chicago, p. 119
Myers P. C., Benson P. J., 1983, ApJ, 266, 309
Myers P. C., Linke R. A., Benson P. J., 1983, ApJ, 264, 517
Myers P. C., Fuller G. A., Matthieu R. D., Beichman C. A., Benson P. J., Schild R. E., Emerson J. P., 1987, ApJ, 319, 340
Parker N. D., 1988, MNRAS, 235, 139
Parker N. D., 1991, MNRAS, 251, 63
Reipurth B., 1983, A&A, 117, 183
Sandqvist Aa., 1977, A&A, 57, 467
Sandqvist Aa., Lindroos K. P., 1976, A&A, 53, 179
Tapia S., 1973, in Greenberg J. M., van de Hulst H. C., eds, Proc. IAU Symp. 52, Interstellar Dust and Related Topics. Reidel, Dordrecht, p. 43
Westin T. N. G., 1985, A&AS, 60, 99
Zealey W. J., Ninkov Z., Rice E., Hartley M., Tritton S. B., 1983, Astrophys. Lett., 23, 119